Research on the EMI Radiation of Discharge of Pantograph-offline on EMU

Yinghong WEN, Bangcheng SUN, Qin WANG, Zhenhui Tan

***Abstract*—Wireless communication plays an important role in high speed railway (HSR) system. As air interface is open, EMI radiation is of significance to HSR wireless communication. This work analyzes current EMI radiation within HSR system firstly, and concludes that main EMI radiation is caused by discharge of Pantograph-offline on EMU. Then on the basis of theoretical models of such discharge, which reflects the physical characteristics of offline signal directly, transient far field radiation model is established and analyzed. Consequently the far field radiation is simulated to verify theoretical model. Results show that, for common wireless communications, such as GSM, LTE and so on, the EMI radiation should be considered in radiation EMS tests for HSR wireless equipments.**

***Index Terms*—HSR; EMI Radiation; Discharge of Pantograph offline;**

I. Introduction

IN the modern high speed railway (HSR) system, various electronic and electrical equipments coexist [1]. To achieve high running speed of electrical multiple units (EMU), relative high power supply is indispensable. Consequently, sizable current exists within HSR system. Furthermore, as the increasing speed of EMU, vibration will introduce offline between pantograph and catenaries (PCO). And such offline introduces sudden changes of current with HSR system. According to basic EM theory, broadband EM radiation occurs as PCO.

Wireless communication plays an important role in HSR system. As air interface is open, EMI radiation of PCO is of significance to HSR wireless communication [2].

Due to the complexity of the environment in HSR, the PCO signal is of great randomness and uncertainty. The existing literatures and measurements show that the PCO signal between locomotive pantograph and contact line is mainly pulse electromagnetic disturbance [3]. The spectrum of the spark discharge is particularly wide which ranges from tens of kHz to GHz [4]. It's difficult to formulate such PCO signals and the EMI radiation in different conditions [5].

This work uses onsite-measured discharge current of PCO, to model and calculate the EMI radiation for EMU. Section II proposes a mathematical model of PCO discharge and lightning current, based on measured data. Then section III calculates the radiated EM field of PCO discharge and lightning current; section IV compares EMI radiation under different conditions, and analyzes characteristics of PCO EMI radiation; finally section V draws conclusions.

II. Model of PCO Discharge Current

During the operation of EMU, once the offline between pantograph and catenary occurs due to vibrations, voltage and current in the contact line tends to breakdown the surrounding air, and generates PCO discharge. Obviously such discharge current depends on status of EMU. And pure theoretical analysis is rather difficult.

According to onsite measurements, PCO discharge occurs several times during one PCO. Such discharges are of several micro-seconds duration, and 10ms interval within time domain. The following Fig. 1 shows the full shape of one PCO discharge current, with vertical axis for current amplitude, and horizontal axis for discharging time.

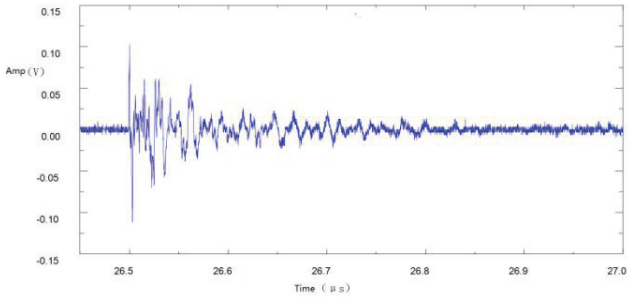

Fig. 1. Pulse amplitude for single pulse signal waveform

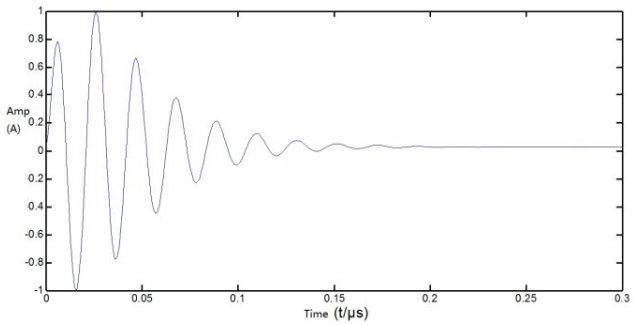

Fig. 2. Normalized current pulse waveform with Eq. (1)

This work is supported by NSFC key project (U1234205), Chinese railway ministry S&T project (2013X001-A-2), and Chinese PHD fund (20120009110005).

Yinghong WEN, is with School of Electronic Information Engineering, Beijing jiaotong University, Beijing, china. (e-mail: yhwen@bjtu.edu.cn).

Bangcheng SUN, is with School of Electronic Information Engineering, Beijing jiaotong University, Beijing, china.

978-1-4673-5710-4/13/$31.00 ©2013 IEEE

As the PCO charges are of the similar mechanism as electrostatic and thunderbolt discharges [6], we use a combination of pulse and sine function to model PCO charge current as follows,

$$i(t) = I_0(1-e^{-t/\alpha})^{\gamma} e^{-\beta t} \sin \omega t \tag{1}$$

According to Fig. 1, the parameters are normalized fixed as following, $I_0 = 1$, $\alpha = 0.04$, $\beta = 4*10^7$, $\gamma = 0.7$. And the current pulse is figured out as Fig. 2.

Comparing Fig. 1 and 2, Eq. (1) can simulate PCO discharge current quite accurately.

III. Transient EMI Radiation of PCO Charges

Consider pantograph catenary vibration equation first [7],

$$l(x,t) = \frac{2p_0 L}{m\pi^2(C_p^2 - v^2)} \sum_{n=1}^{\infty} \frac{1}{n^2} \sin\frac{n\pi x}{L} \left(\sin\frac{n\pi v t}{L} - \frac{v}{C_p}\sin\frac{n\pi C_p t}{L}\right) \tag{2}$$

Where, m denotes per length-unit mass of catenary; C_p denotes the speed of vibrating wave travelling along catenary; p_0 denotes lifting force of pantograph moving with speed of v; and L denotes span of catenary. Considering the parameters of EMU, $l(x, t)$, the gap between pantograph and catenary, is commonly 10^{-2} order of magnitude.

Firstly, consider the free space case. This is modeled as the following Fig. 3, under XYZ coordinate system.

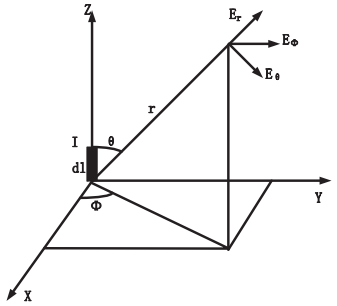

Fig. 3. The dipole model

Darren Bell equation gives the scalar and vector potential functions as below,

$$\begin{cases} \phi(\vec{r},t) = \dfrac{1}{4\pi\varepsilon}\displaystyle\int_{\tau} \frac{\rho(\vec{r}')e^{j\omega(t-\frac{R}{v})}}{R} d\tau \\ \vec{A}(\vec{r},t) = \dfrac{\mu}{4\pi}\displaystyle\int_{\tau} \frac{\vec{J}(\vec{r}')e^{j\omega(t-\frac{R}{v})}}{R} d\tau \end{cases} \tag{3}$$

Then magnetic vector potential can be simplified under sphere coordinate system as,

$$\vec{A}(\vec{r},t) \approx \vec{a}_z \frac{\mu l(x,t)}{4\pi}\frac{e^{-j\beta r}e^{j\omega t}}{r} i(t) = i(t)l(x,t)\frac{\mu}{4\pi r}e^{-j\beta r}e^{j\omega t}(\vec{a}_r\cos\theta - \vec{a}_\theta \sin\theta) \tag{4}$$

Where, β is wave factor,

$$\beta = w\sqrt{\mu\varepsilon} \tag{5}$$

Under Lorentz regulation, magnetic field is computed as follows,

$$H(\vec{r},t) = \frac{1}{\mu}\nabla\times\vec{A}(\vec{r},t) = \vec{a}_\phi i(t)l(x,t)\frac{\mu}{4\pi}e^{-j\beta r}\left(\frac{j\beta}{r} + \frac{1}{r^2}\right)e^{j\omega t}\sin\theta \tag{6}$$

Consider the point of $\vec{r}$ as passive area, for there is neither electric charge nor current. Then Maxwell equation is degenerated into,

$$\begin{cases} \nabla\times H = j\omega D \\ \nabla\times E = -j\omega B \\ \nabla\cdot D = 0 \\ \nabla\cdot B = 0 \end{cases} \tag{7}$$

So we have transient electric field.

$$\vec{E}(\vec{r},t) = \frac{1}{j\omega\varepsilon}\nabla\times\vec{H}(\vec{r},t) = \frac{i(t)l(x,t)}{2\pi\omega\varepsilon}e^{-j\beta r}e^{j\omega t}\begin{bmatrix} \vec{a}_\theta \dfrac{1}{2}\left(j\dfrac{\beta^2}{r} + \dfrac{\beta}{r^2} - j\dfrac{1}{r^3}\right)\sin\theta \\ +\vec{a}_r\left(\dfrac{\beta}{r^2} - j\dfrac{1}{r^3}\right)\cos\theta \end{bmatrix} \tag{8}$$

When it comes to radiated EMI, it means that we only consider far field. So we have radiated EMI for PCO charge within free space as,

$$\begin{cases} H(\vec{r},t) = j\vec{a}_\phi \dfrac{\mu\dot{i}(t)l(x,t)\beta}{4\pi r}\sin\theta e^{-j\beta r}e^{j\omega t} \\ \vec{E}(\vec{r},t) = j\vec{a}_\theta \dfrac{i(t)l(x,t)\beta^2}{4\pi\omega\varepsilon r}\sin\theta e^{-j\beta r}e^{j\omega t} \end{cases} \tag{9}$$

Comparing to size of EMU, such PCO current can be seen as a time varying current dipole over an infinite plane of the conductor. Consequently, EMI radiation is computed with image theory, shown as Fig. 4.

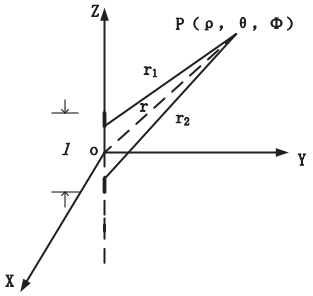

Fig. 4. The sketch drawing of dipole and the site

According to image theory, PCO current and its image form an antenna array. And the factor of such array is,

$$F(\theta) = \cos\left(\frac{\beta d}{2}\cos\theta\right) \tag{10}$$

Where, d denotes the distance from PCO current to the top of EMU. According to multiplication principle of antenna array factor, we have PCO transient EMI radiation within EMU as follows,

$$\begin{cases} H(\vec{r},t) = j\vec{a}_\phi \dfrac{\mu i(t) l(x,t)\beta}{4\pi r} \cos(\dfrac{\beta d}{2}\cos\theta)\sin\theta e^{-j\beta r} e^{j\omega t} \\ \vec{E}(\vec{r},t) = j\vec{a}_\theta \dfrac{i(t) l(x,t)\beta^2}{4\pi\omega\varepsilon r} \cos(\dfrac{\beta d}{2}\cos\theta)\sin\theta e^{-j\beta r} e^{j\omega t} \end{cases} \quad (11)$$

IV. Measurements and Verifications

The onsite measurement is achieved with EMU of 8 units, which is of 201.4m length. And pantographs are located on the top of 4th and 6th EMU units. The EMU runs with only one pantograph, at a maximum speed of 350km/h.

TABLE I
The Test Equipment

Equipment	Version	Parameter
Digital oscilloscope	Tektronix DPO7354	Bandwidth of 3.5GHz, Sampling rate of 50Gs/s
Electric field probe	EMCO 7405: 904B	30MHz-3GHz

Electric field probe is located 0.4m up to the top of EMU, and 2.5m beside the contact between pantograph and catenary.

Considering the EMI characteristics within frequency domain, the onsite measuring data is figured out in the following Fig. 5 (a). Also Fig. 5 (b) demonstrates the theoretical results based on Eq. (11).

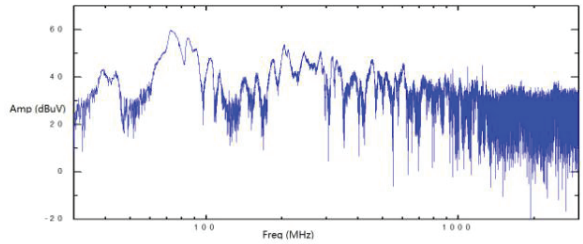

Fig. 5 (a). EMI characteristics of onsite measurements

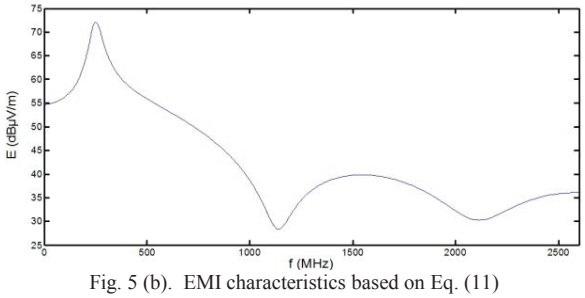

Fig. 5 (b). EMI characteristics based on Eq. (11)

The theoretical model of Eq. (11) can quite accurately profile the envelope of the onsite measurements. And this verifies the proposed theoretical model of Eq. (11).

V. Analysis on EMI Radiation of PCO Charges

This section analyzes the EMI radiation of PCO charge with theoretical model shown as Eq. (11).

A. Simulation Model

The proposed theoretical model of Eq. (11) is simulated with FDTD software. The simulation model is shown as Fig. 6.

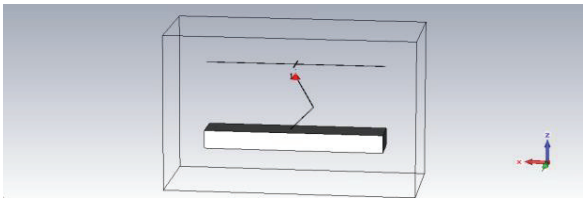

Fig. 6. Model in electromagnetic FDTD software

B. EMI Variation with Distance

Variation of electric and magnetic field with the observing point and the source point radial distance *r* is as shown in Fig. 7 (a) and (b).

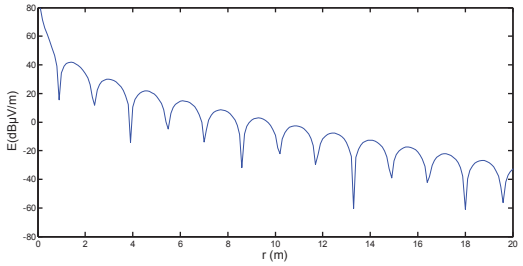

Fig. 7 (a). Variation of electric field with Distance

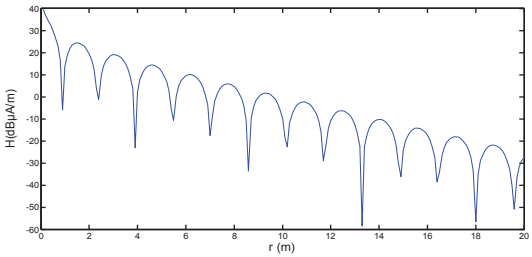

Fig. 7 (b). Variation of magnetic field with Distance

Electric field is of faster attenuation with increasing distance than magnetic field. And a distance of 4m seems to be a milestone, the EMI radiation becomes very tiny farther than 4m.

C. EMI Envelope Variation with Time

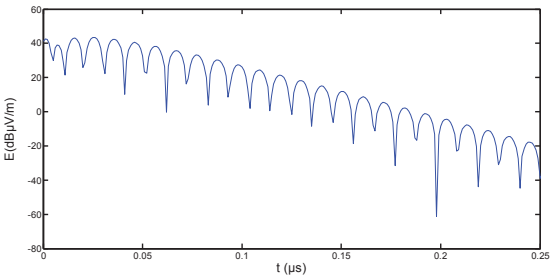

Fig. 8 (a). Variation of electric field with Time at *r* = 1.5m

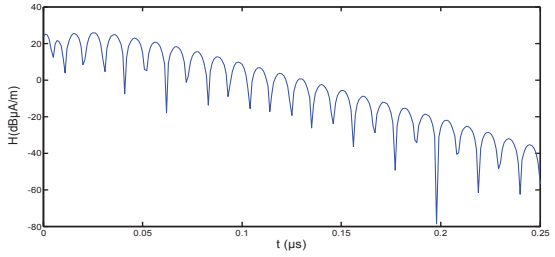

Fig. 8 (b). Variation of magnetic field with Time at *r* = 1.5m

Choose the distance of 1.5m to see the variation of electric

and magnetic field with time. The results are shown in Fig. 8 (a) and (b).

The electric field from time zero after the surge, with time in vibration attenuation trend until 100 ns is very weak, the pantograph offline signal source in the (r=1.5m) of the electric field effect is not obvious.

The magnetic field from zero time increases, the oscillation characteristics of the signal source, was oscillating trend increases with time, and in 50 ns after time decrease, in 100 ns, the pantograph offline signal source at the point (r=1.5m) field effect is very weak.

VI. CONCLUSIONS

This work analyzes current EMI radiation within HSR system firstly, and concludes that main EMI radiation is caused by discharge of Pantograph-offline on EMU. Then on the basis of theoretical models of such discharge, which reflects the physical characteristics of offline signal directly, transient far field radiation model is established and analyzed. Consequently the far field radiation is simulated to verify theoretical model. Results show that, for common wireless communications, such as GSM, LTE and so on, the EMI radiation should be considered in radiation EMS tests for HSR wireless equipments.

REFERENCES

[1] Yong-jian Zhi, Bin Zhang, Kai Li, Xiao-yan Huang, You-tong Fang, Wen-ping Cao. Electromagnetic environment around a high-speed railway using analytical technique[J]. Journal of Zhejiang University-Science A(Applied Physics & Engineering),2011(12)：950-956

[2] C. Sharma, V. Fotheringham. Wideband 3G to Broadband 4G:Collision and Convergence of Standards[J]. Wireless Broadband:Conflict and Convergenc, pp.167-189, 2008

[3] Anonymous. Research and Markets on Long Term Evolution 2009 - the Role of LTE in Mobile Wireless Networks through 2015[J]. Network Weekly News, 2009

[4] Jaime Calle-Sánchez, Mariano Molina-García, José I. Alonso, Alfonso Fernández-Durán. Long Term Evolution in High Speed Railway Environments: Feasibility and Challenges[J]. Bell Labs Technical Journal, 2013

[5] Michael Liem and Veena B. Mendiratta. Mission Critical Communication Networksfor Railways[J]. Bell Labs Technical Journal, 2011.

[6] Keenan R K,Keenan R K, Rosi L A, et al. Some fundamental aspects of ESD testing(part1). Proc IEEE International Symposium on Electro-magnetic Compatibility. 1991,236-241.

[7] Berghe S V D,Beyghe S V D, Zutter D, et al. Study of ESD signal entry through coaxial cable shields[J].Journal of Electrostatic. 1998,44:135-148.

Yinghong WEN, PHD., and professor, is with School of Electronic Information Engineering, Beijing jiaotong University, Beijing, china. And her major researches are focused on EMC within HSR.